Electronic supplementary information

Novel Neutral Guest Recognition and Interpenetrated Complex Formation from Pillar[5]arenes

Chunju Li, Songhui Chen, Jian Li, Kang Han, Min Xu, Bingjie Hu, Yihua Yu, and Xueshun Jia

cjli@shu.edu.cn

Contents

Materials and methods.

n-Butyl imidazol was commercially available and used as received. Bis(imidazol) derivatives[1] (BImBu, BImPro, BImPen, and BImBn) were prepared by literature methods and recrystallized and dried under reduced pressure before use. AlkP5A hosts[2] (MeP5A, EtP5A, BuP5A and OctP5A) were prepared by condensation of the corresponding 1,4-dialkoxybenzene with paraformaldehyde and $BF_3{\cdot}O(C_2H_5)_2$ as a catalyst. ^{1}H NMR, ^{13}C NMR and 2D NOESY spectra were recorded on a Bruker AV500 instrument.

Copies of ^{1}H NMR and ^{13}C NMR spectra of hosts and guests.

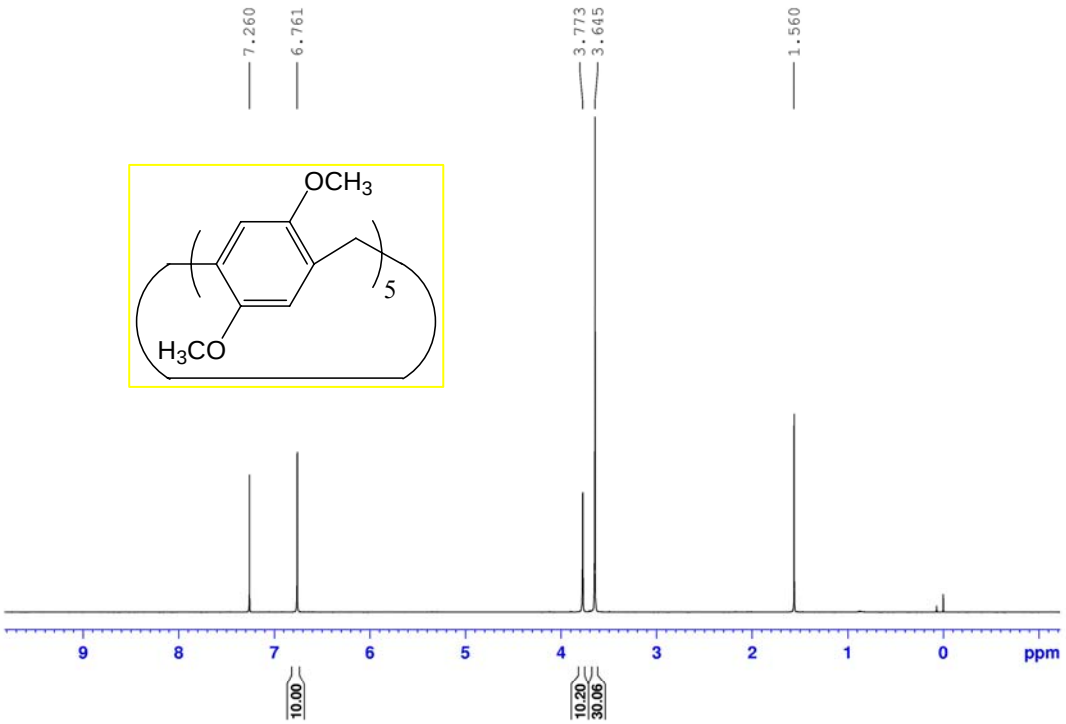

Figure S1. ^{1}H NMR spectrum (500 MHz) of MeP5A in $CDCl_3$.

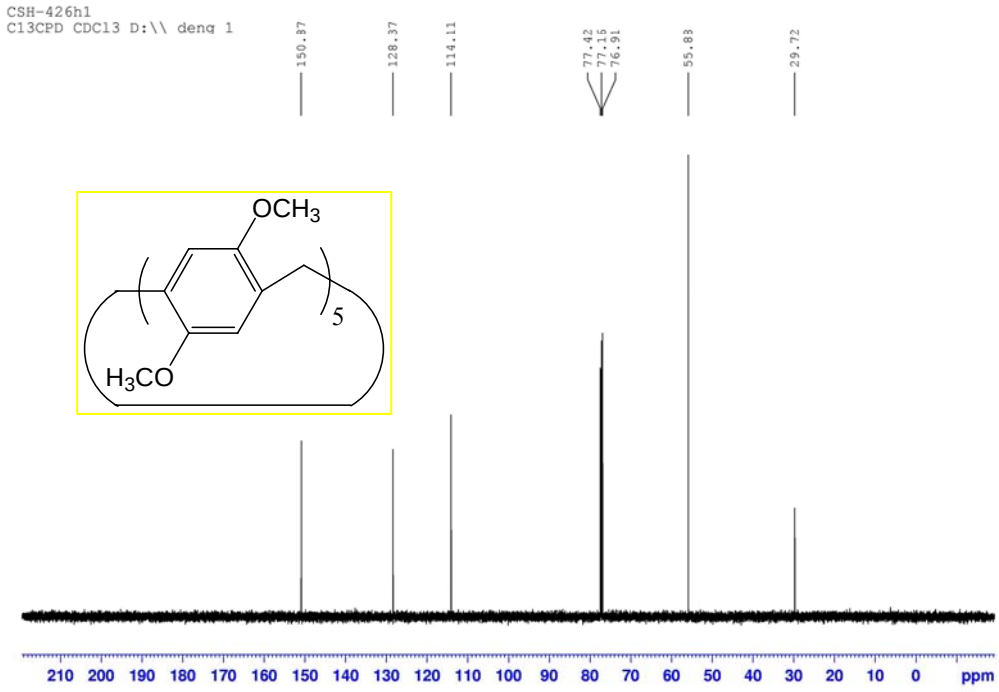

Figure S2. ^{13}C NMR spectrum (125 MHz) of MeP5A in $CDCl_3$.

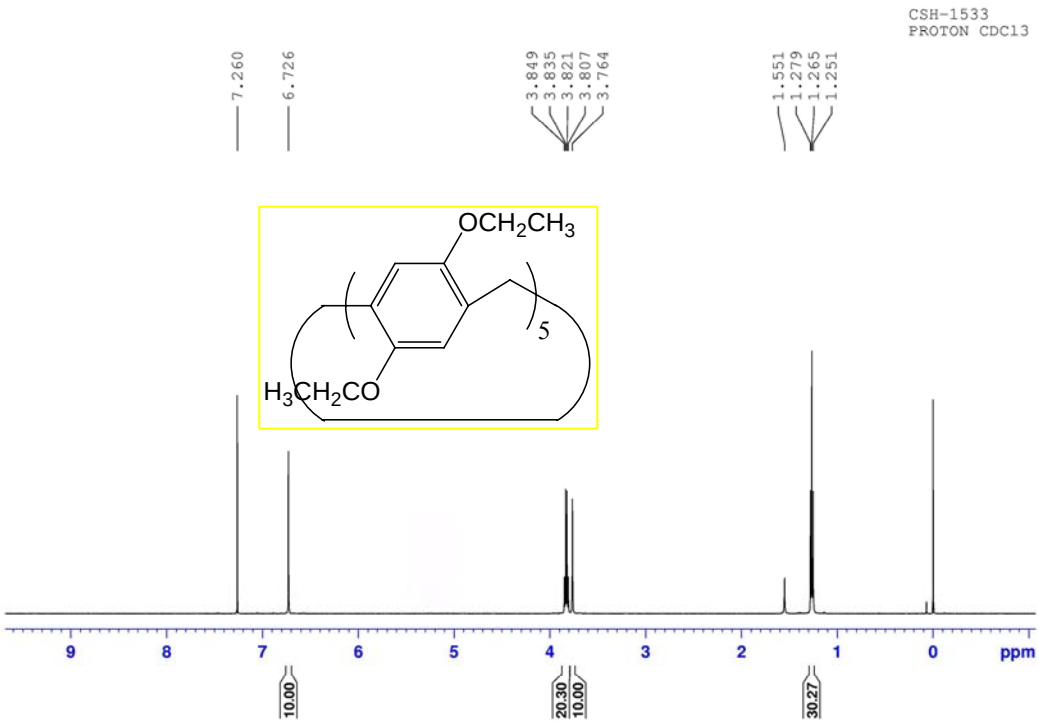

Figure S3. ^{1}H NMR spectrum (500 MHz) of EtP5A in $CDCl_3$.

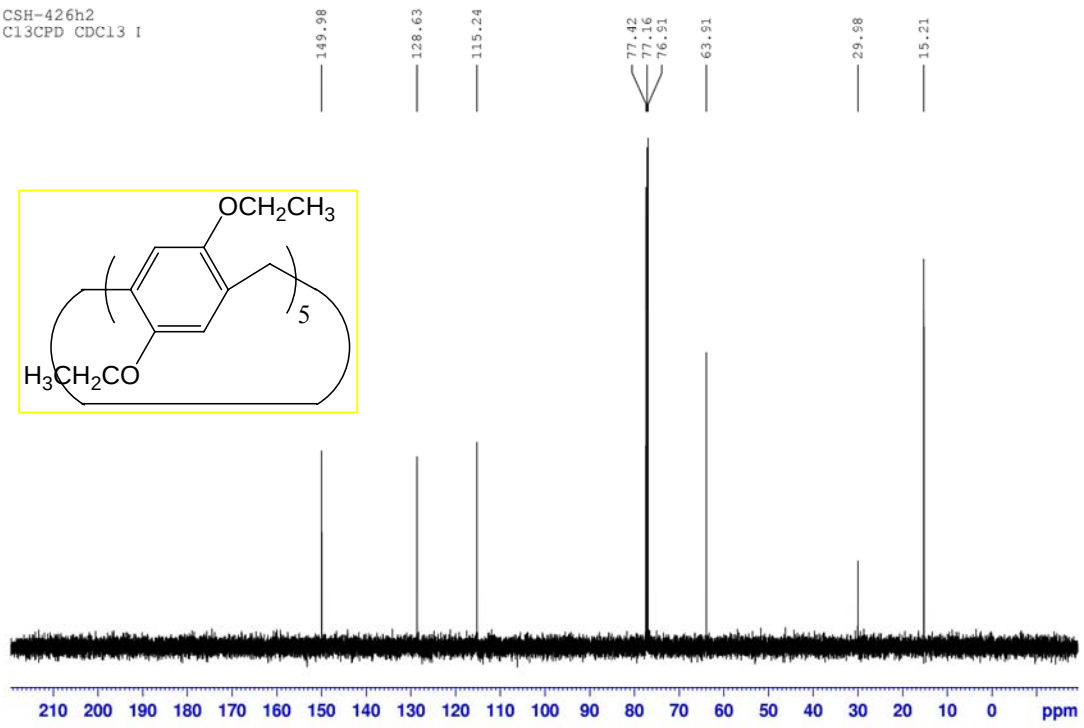

Figure S4. ^{13}C NMR spectrum (125 MHz) of EtP5A in $CDCl_3$.

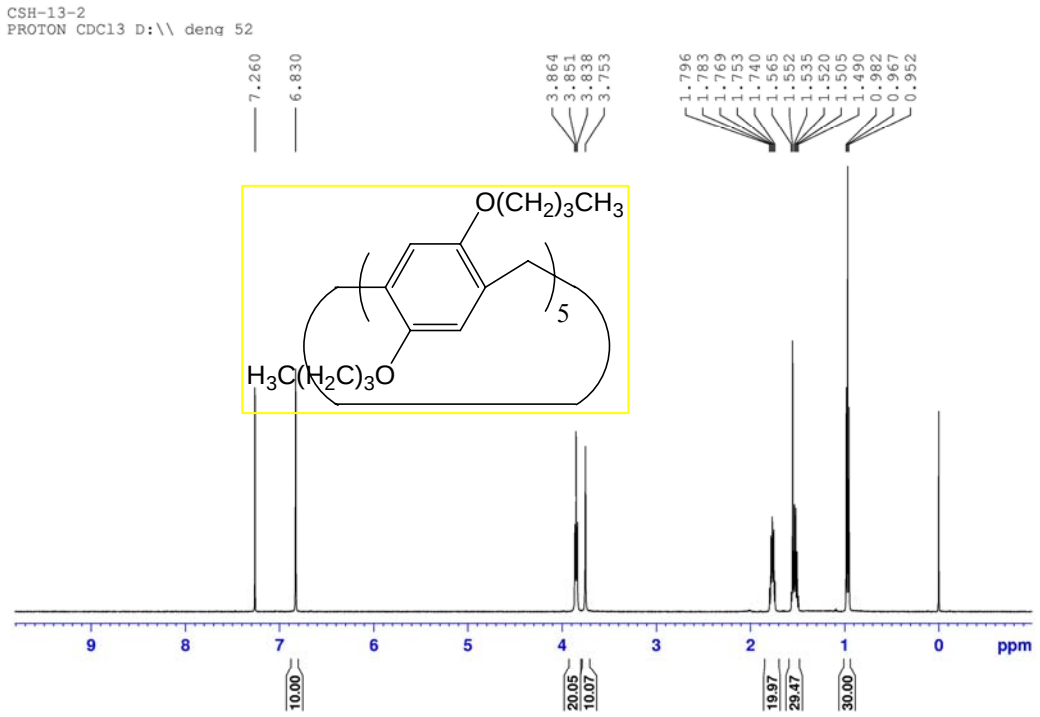

Figure S5. ^{1}H NMR spectrum (500 MHz) of BuP5A in $CDCl_3$.

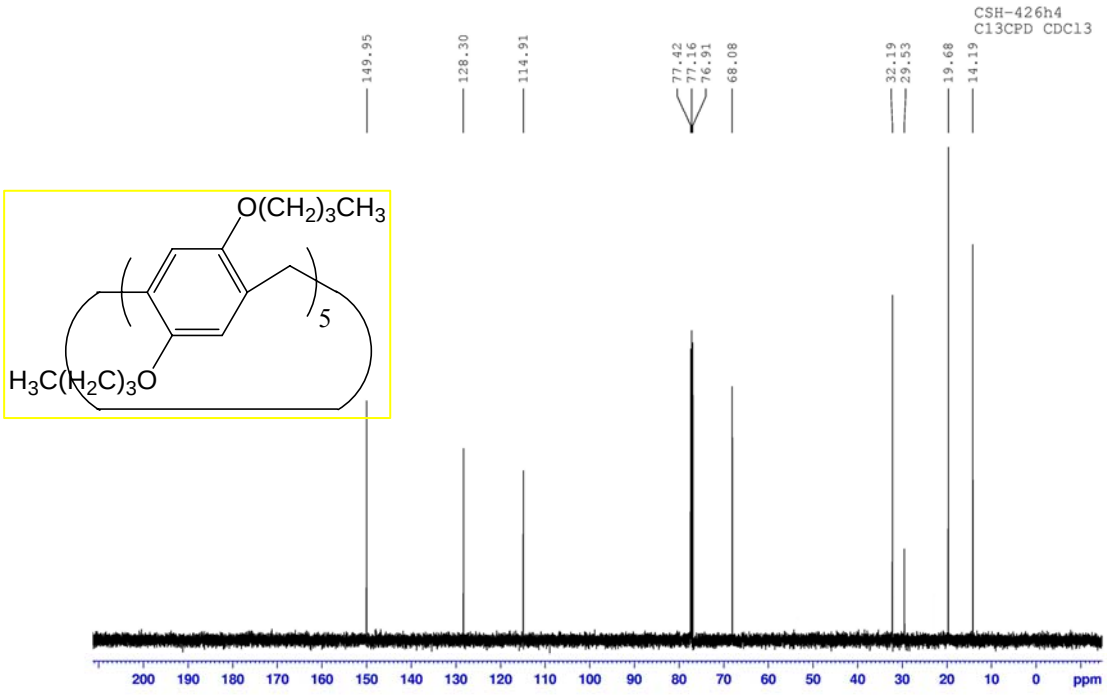

Figure S6. ^{13}C NMR spectrum (125 MHz) of BuP5A in $CDCl_3$.

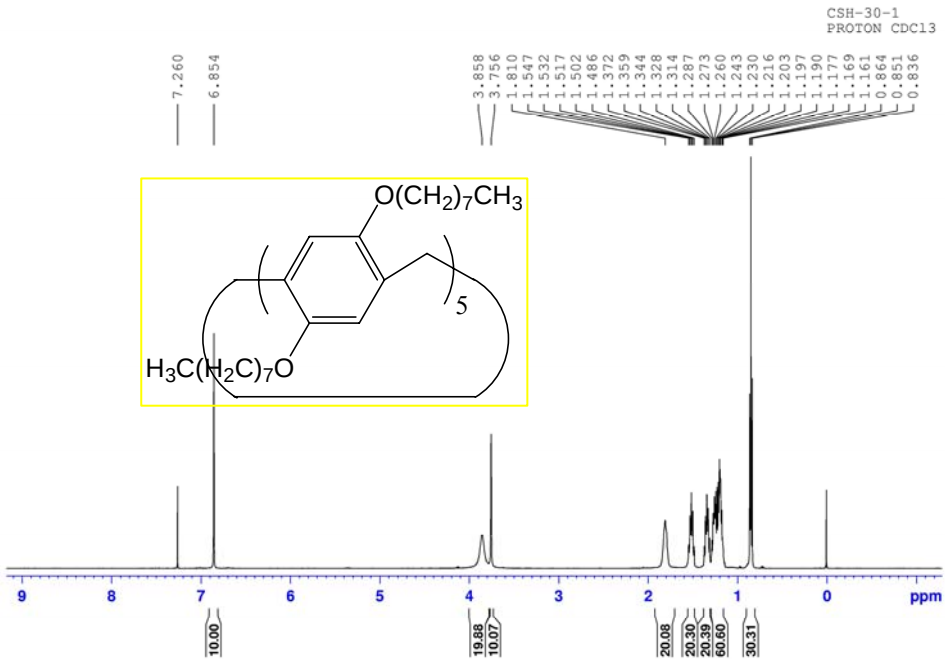

Figure S7. ^{1}H NMR spectrum (500 MHz) of OctP5A in $CDCl_3$.

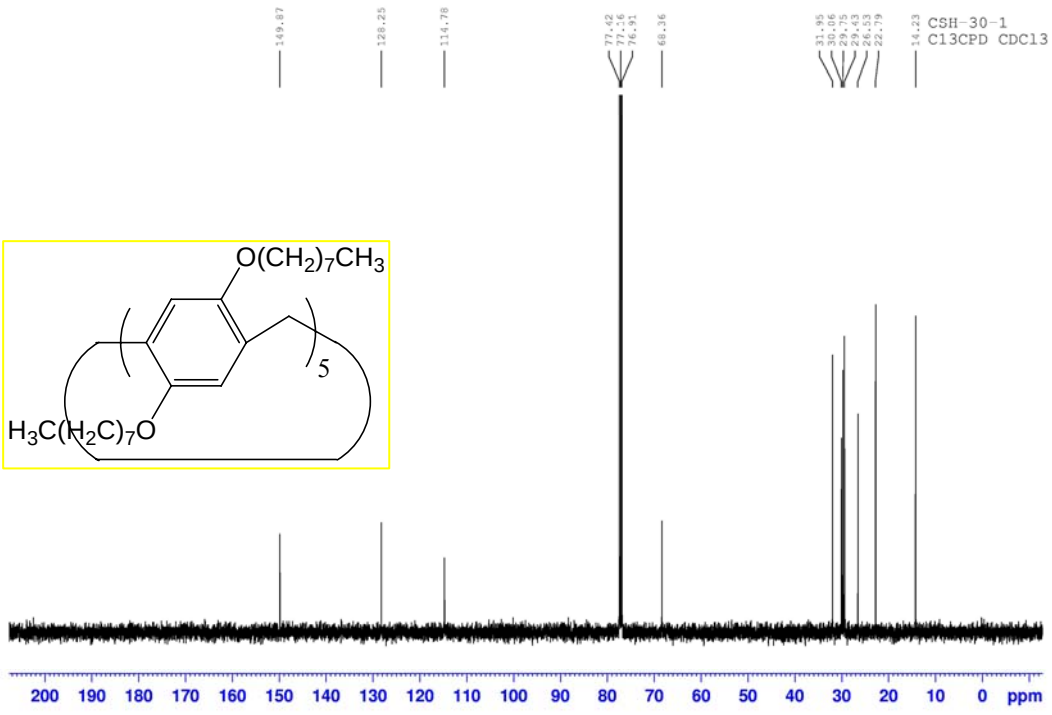

Figure S8. ^{13}C NMR spectrum (125 MHz) of OctP5A in $CDCl_3$.

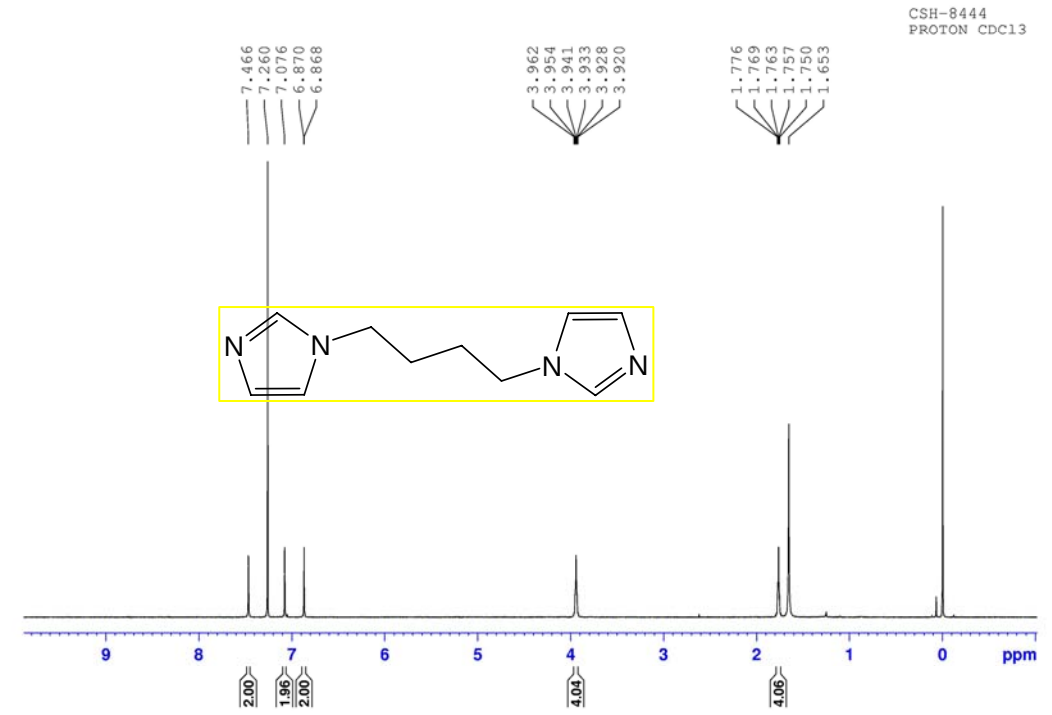

Figure S9. ^{1}H NMR spectrum (500 MHz) of BImBu in $CDCl_3$.

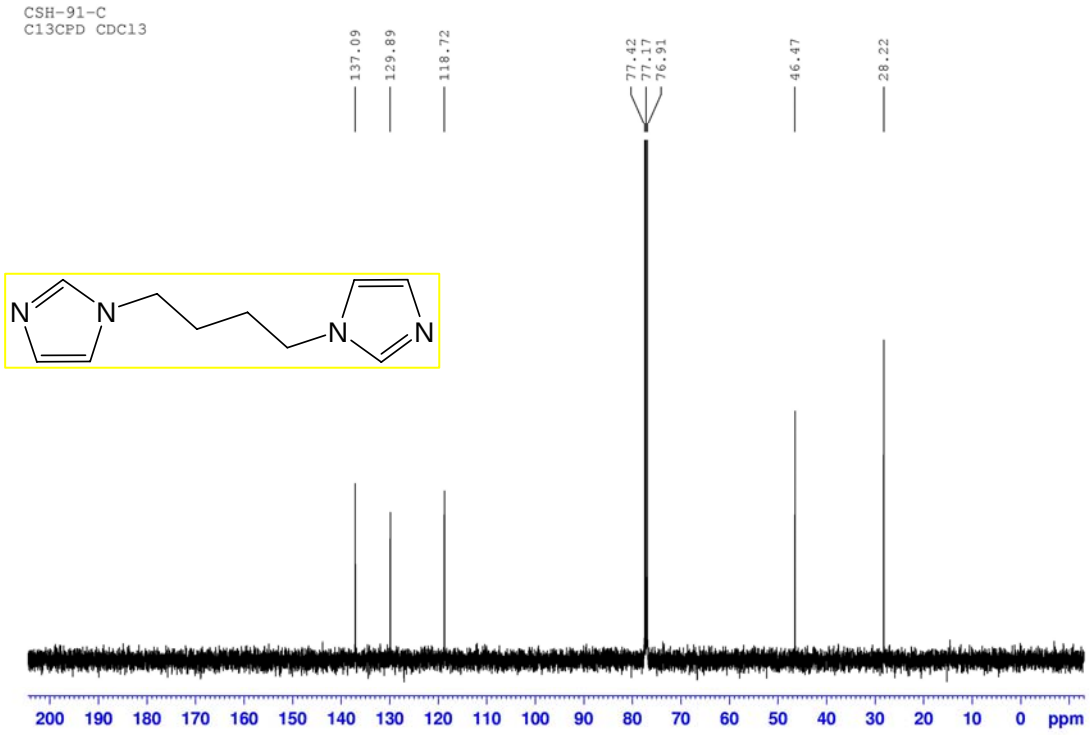

Figure S10. ^{13}C NMR spectrum (125 MHz) of BImBu in $CDCl_3$.

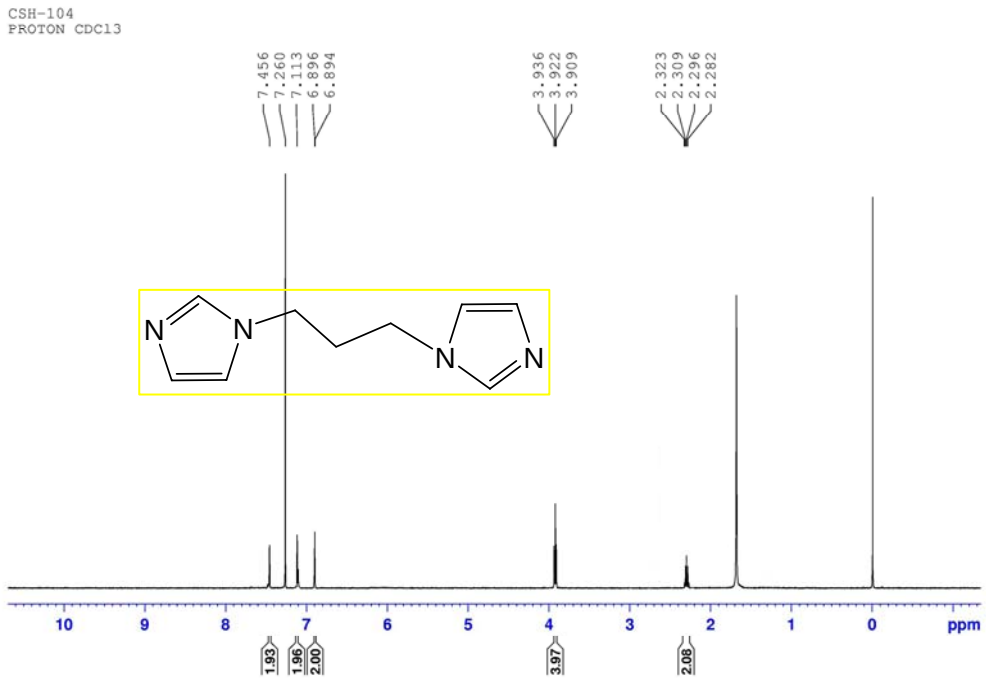

Figure S11. ^{1}H NMR spectrum (500 MHz) of BImPro in $CDCl_3$.

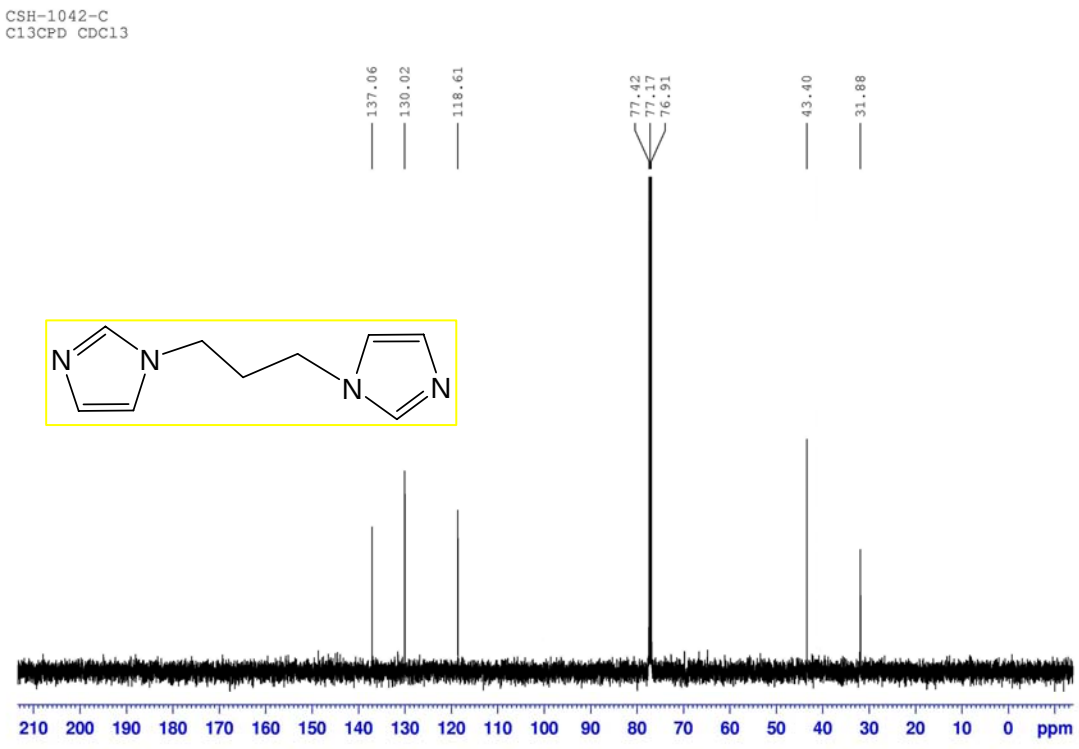

Figure S12. ^{13}C NMR spectrum (125 MHz) of BImPro in $CDCl_3$.

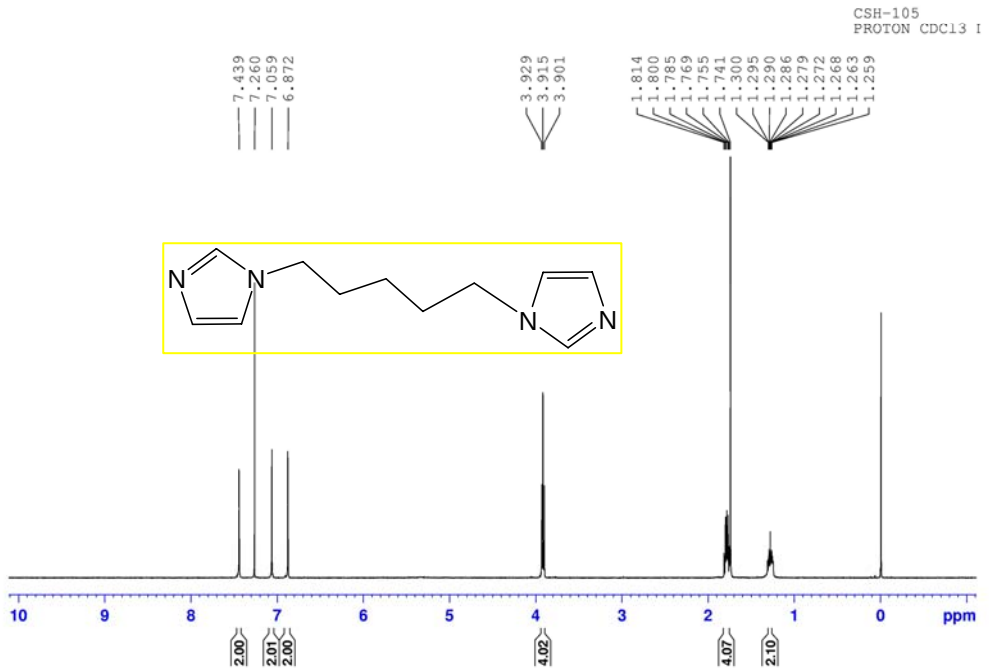

Figure S13. ^{1}H NMR spectrum (500 MHz) of BImPen in $CDCl_3$.

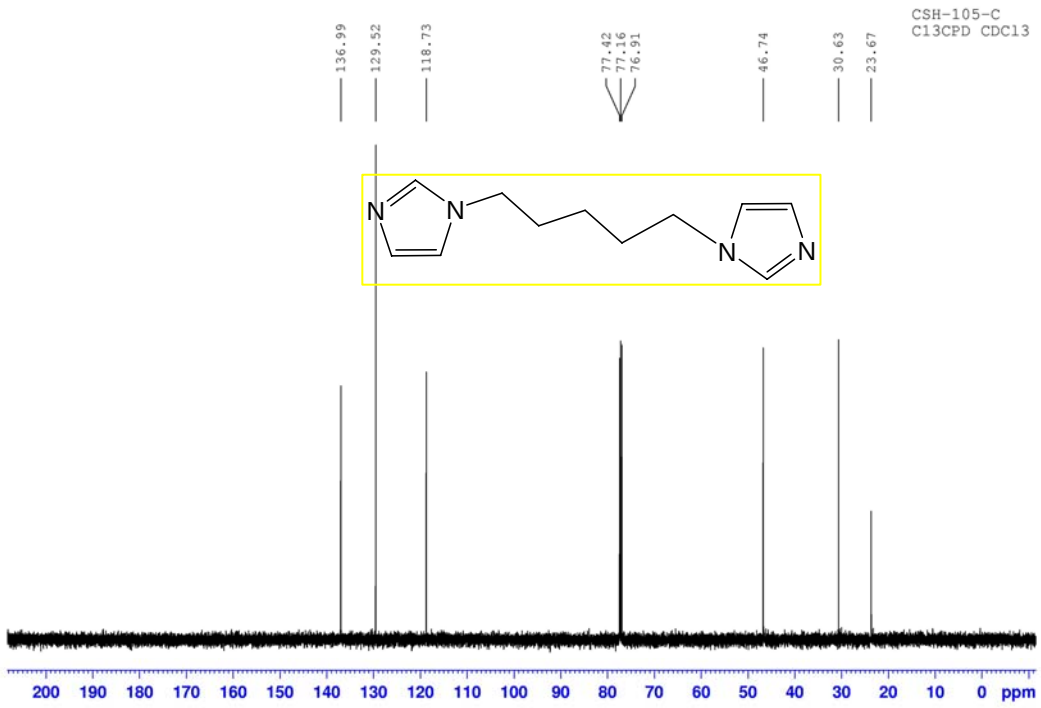

Figure S14. ^{13}C NMR spectrum (125 MHz) of BImPen in $CDCl_3$.

Figure S15. ^{1}H NMR spectrum (500 MHz) of BImBn in $CDCl_3$.

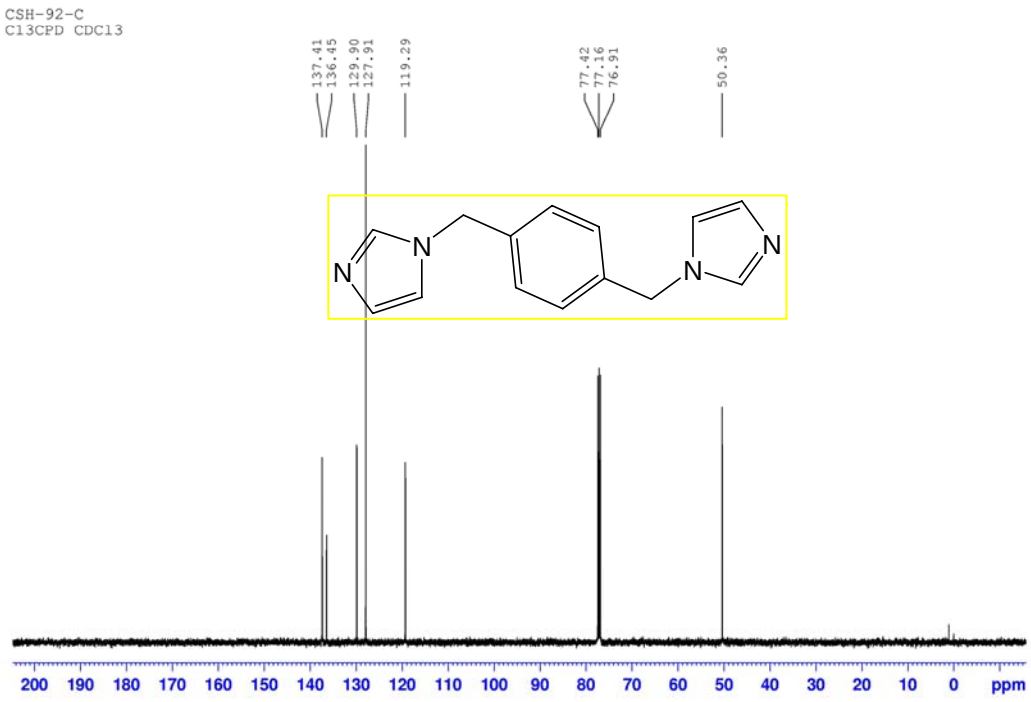

Figure S16. ^{13}C NMR spectrum (125 MHz) of BImBn in $CDCl_3$.

^{1}H NMR spectra of guests in the absence and presence of AlP5As.

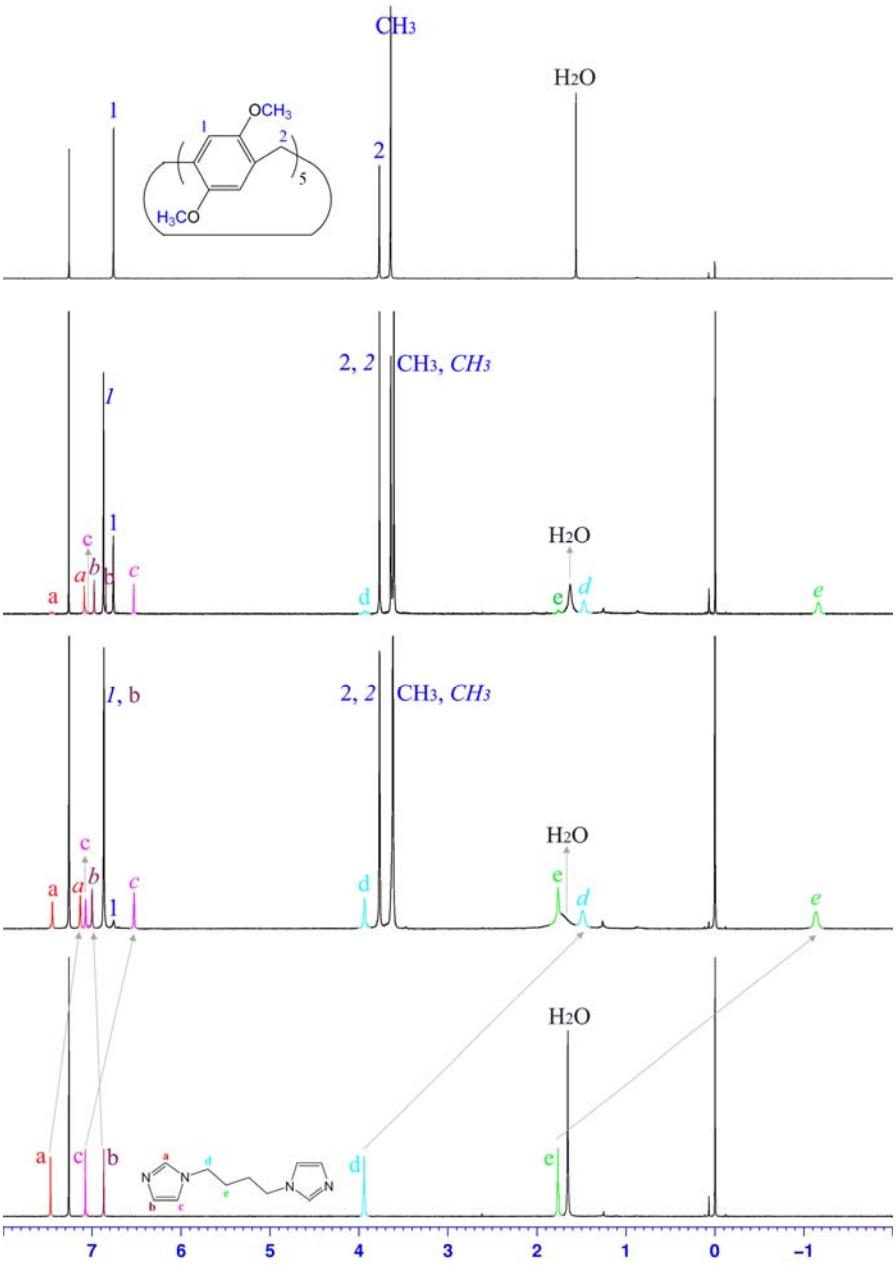

Figure S17. ^{1}H NMR spectra of BImBu (4.2 mM, 500 MHz, $CDCl_3$) in the presence of increasing amounts of MeP5A; from bottom to top: 0.0, 0.6, and 1.3 equivalents. For comparison, the spectrum of the uncomplexed MeP5A is shown at the top. Italics represent complexed host and guest.

Notice that a new species occurs, in addition to the corresponding signals for the uncomplexed axle and wheel, indicating slow exchange on the NMR timescale. The peaks for methylene protons (H_d and H_e) and the α-protons of the imidazol N_1 atom (H_a and H_c) of BImBu exhibit substantial upfield shifts. While the β-protons (H_b) shifts slightly downfield. The resonances of the new species are consistent with the formation of an interpenetrated complex.

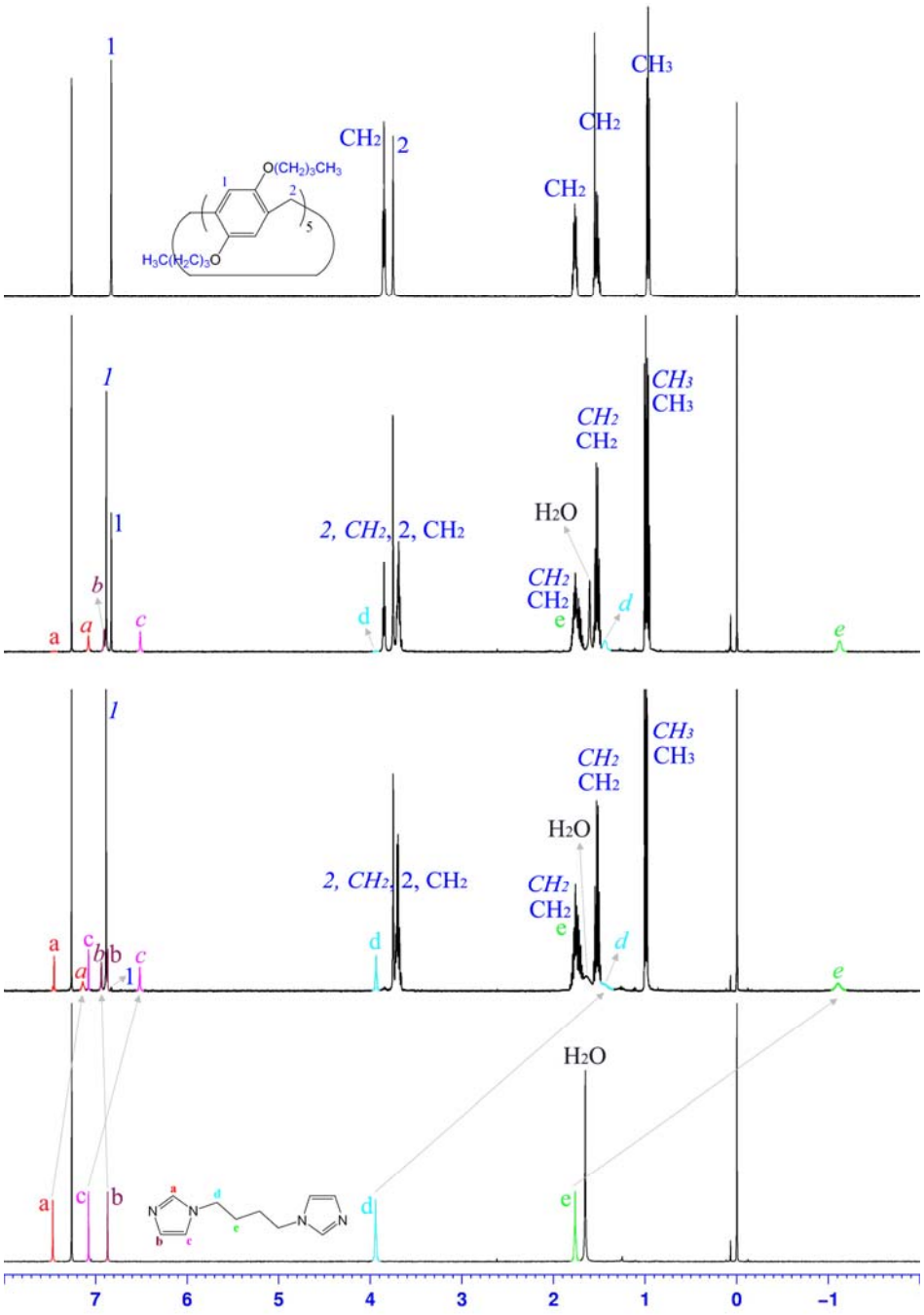

Figure S18. ^{1}H NMR spectra of BImBu (4.2 mM, 500 MHz, $CDCl_3$) in the presence of increasing amounts of BuP5A; from bottom to top: 0.0, 0.6, and 1.2 equivalents. For comparison, the spectrum of the uncomplexed BuP5A is shown at the top. Italics represent complexed host and guest.

Notice that a new species occurs, in addition to the corresponding signals for the uncomplexed axle and wheel, indicating slow exchange on the NMR timescale. The peaks for methylene protons (H_d and H_e) and the α-protons of the imidazol N_1 atom (H_a and H_c) of BImBu exhibit substantial upfield shifts. While the β-protons (H_b) shifts slightly downfield. The resonances of the new species are consistent with the formation of an interpenetrated complex.

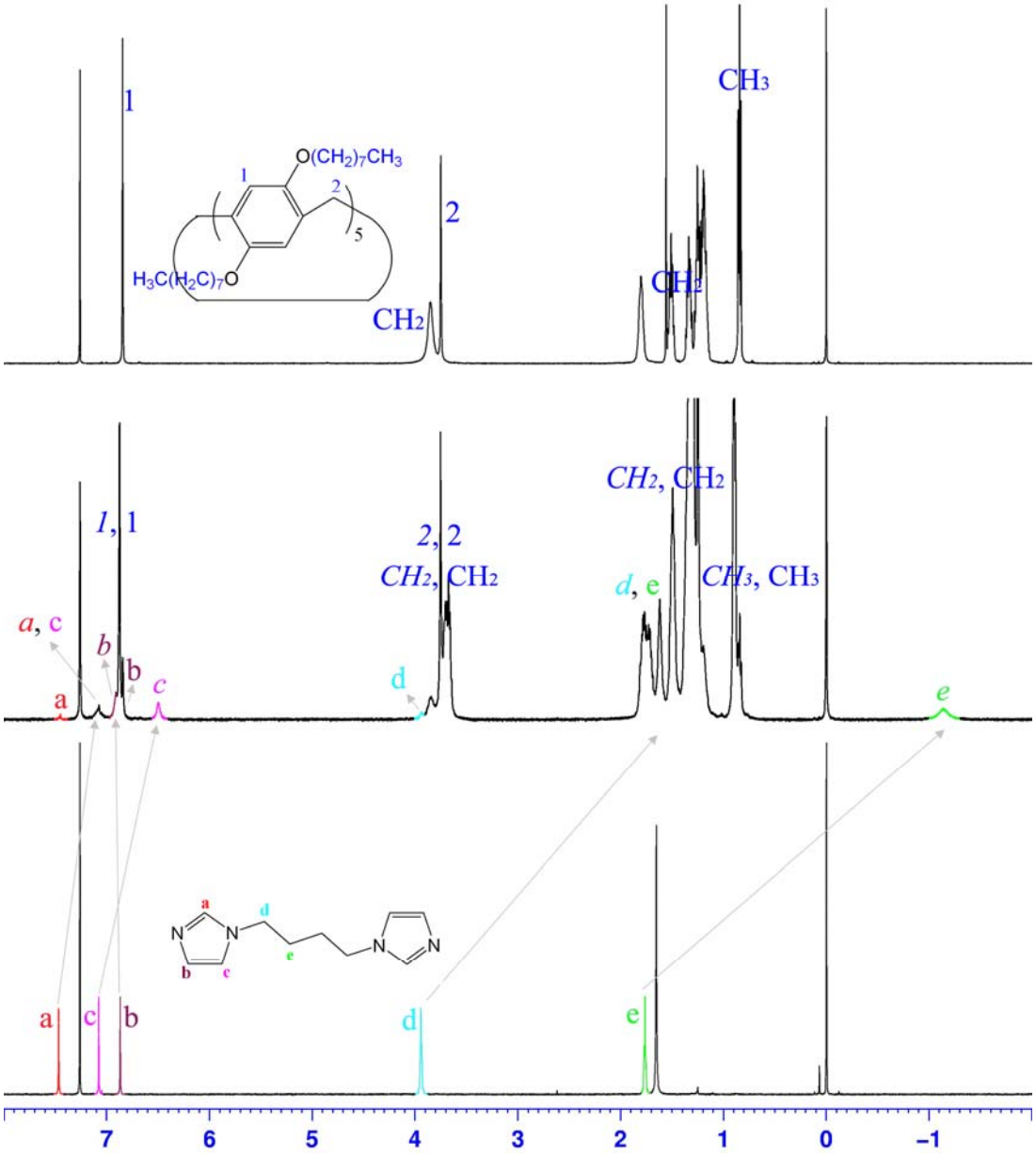

Figure S19. ^{1}H NMR spectra of BImBu (4.2 mM, 500 MHz, $CDCl_3$) in the presence of OctP5A; from bottom to top: 0.0, and 1.2 equivalents. For comparison, the spectrum of the uncomplexed OctP5A is shown at the top. Italics represent complexed host and guest.

Notice that a new species occurs, in addition to the corresponding signals for the uncomplexed axle and wheel, indicating slow exchange on the NMR timescale. The peaks for methylene protons (H_d and H_e) and the α-protons of the imidazol N_1 atom (H_a and H_c) of BImBu exhibit substantial upfield shifts. While the β-protons (H_b) shifts slightly downfield. The resonances of the new species are consistent with the formation of an interpenetrated complex.

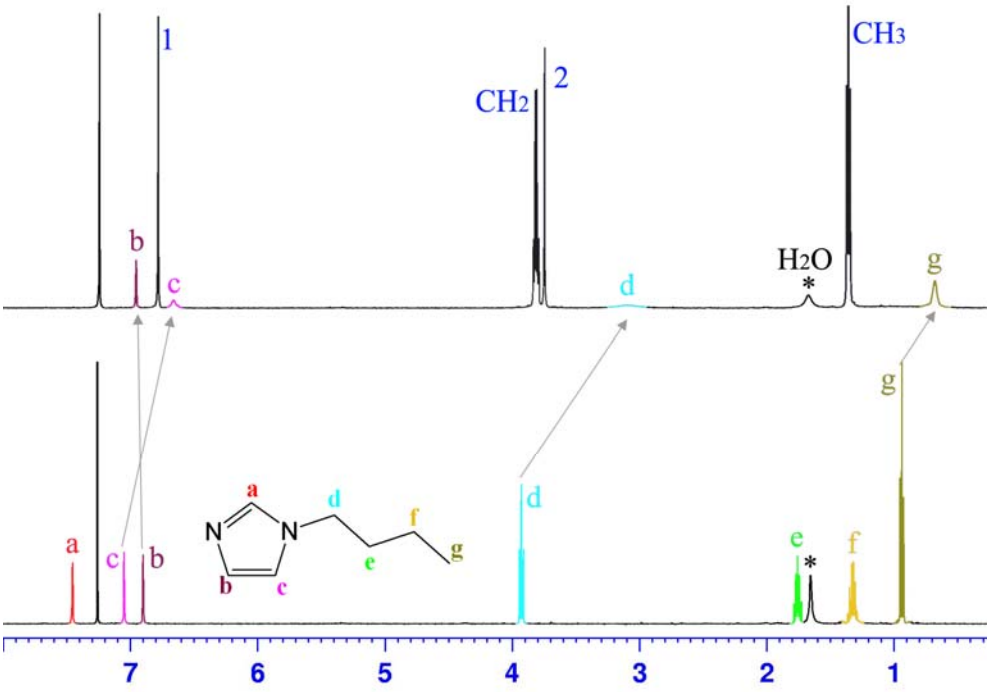

Figure S20. ^{1}H NMR spectrum (500 MHz) of BuIm (4.9 mM) in the absence (lower) and presence (upper) of EtP5A host (5.0 mM) in $CDCl_3$.

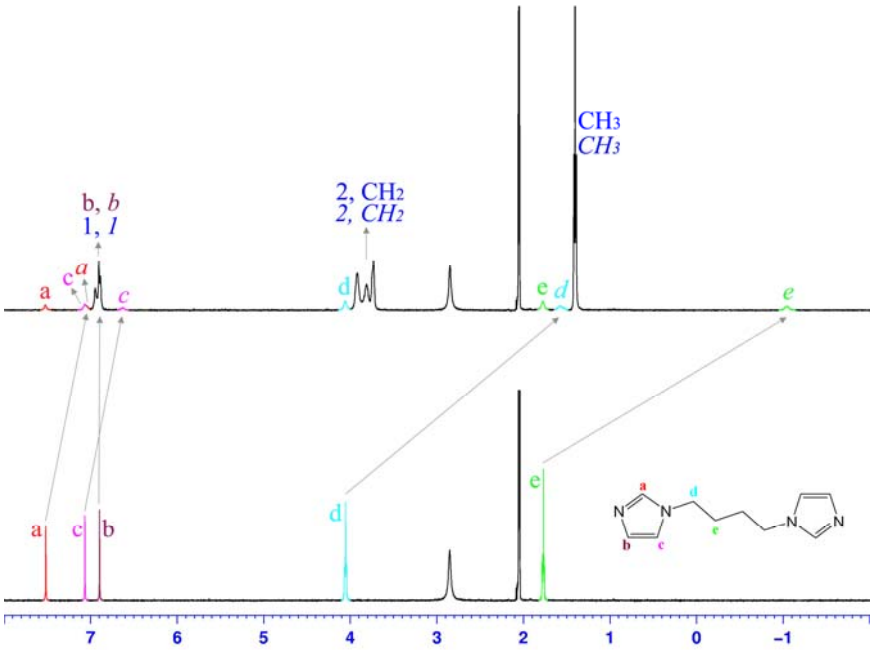

Figure S21. ^{1}H NMR spectrum (500 MHz) of BImBu (4.7 mM) in the absence (lower) and presence (upper) of EtP5A host (5.5 mM) in acetone-d_6.

Notice that a new species occurs, in addition to the corresponding signals for the uncomplexed axle and wheel, indicating slow exchange on the NMR timescale. The peaks for methylene protons (H_d and H_e) and the α-protons of the imidazol N_1 atom (H_a and H_c) of BImBu exhibit substantial upfield shifts. While the β-protons (H_b) shifts slightly downfield. The resonances of the new species are consistent with the formation of an interpenetrated complex.

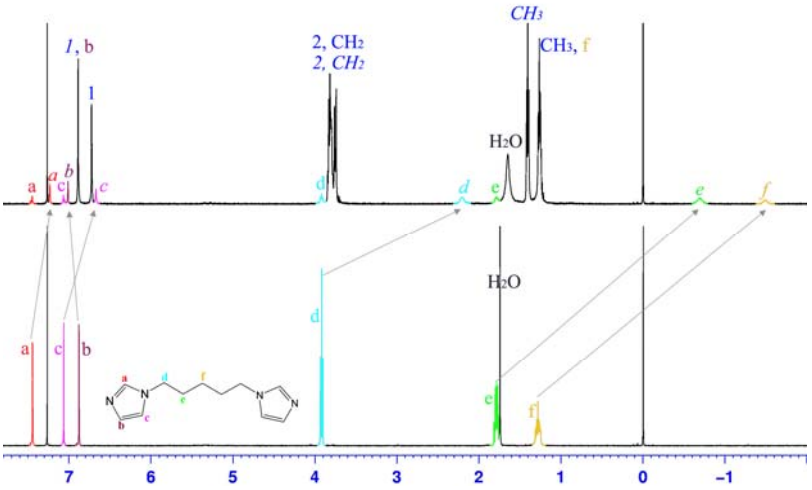

Figure S22. ^{1}H NMR spectrum (500 MHz) of BImBn (4.4 mM) in the absence (lower) and presence (upper) of EtP5A host (5.2 mM) in $CDCl_3$.

Notice that a new species occurs, in addition to the corresponding signals for the uncomplexed axle and wheel, indicating slow exchange on the NMR timescale. The peaks for methylene protons (H_d, H_e and H_f) and the α-protons of the imidazol N_1 atom (H_a and H_c) of BImBu exhibit substantial upfield shifts. While the β-protons (H_b) shifts slightly downfield. The resonances of the new species are consistent with the formation of an interpenetrated complex.

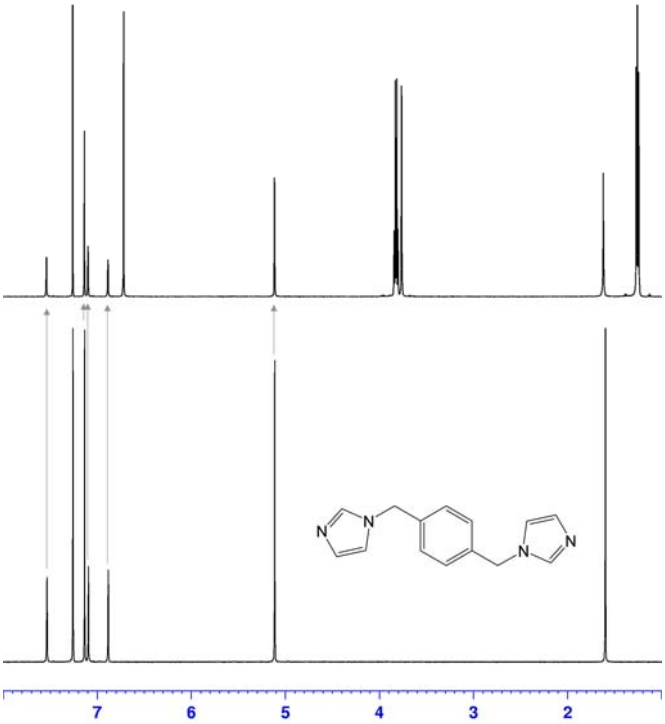

Figure S23. ^{1}H NMR spectrum (500 MHz) of BImBn (5.0 mM) in the absence (lower) and presence (upper) of EtP5A host (5.3 mM) in $CDCl_3$. NMR results indicated that EtP5A did not form inclusion complex with the guest or at least had very weak interactions.

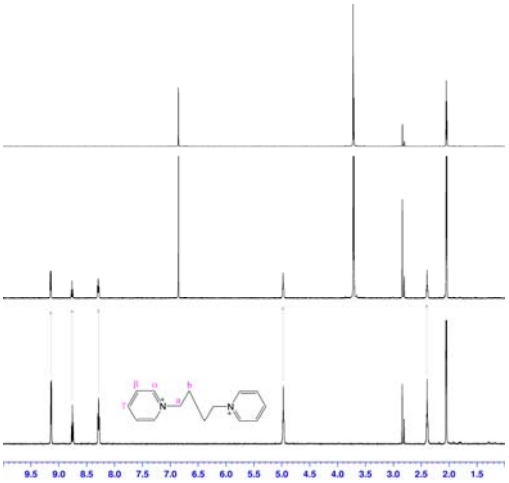

Figure S24. ^{1}H NMR spectra of 1,4-bis(pyridinium)butane bihexafluorophosphate salt (3.2 mM, 500 MHz, $CDCl_3$) in the absence and presence of MeP5A host (3.0 mM). For comparison, the spectrum of the uncomplexed MeP5A is shown at the top. NMR results indicated that MeP5A did not form inclusion complex with the guest or at least had very weak interactions.

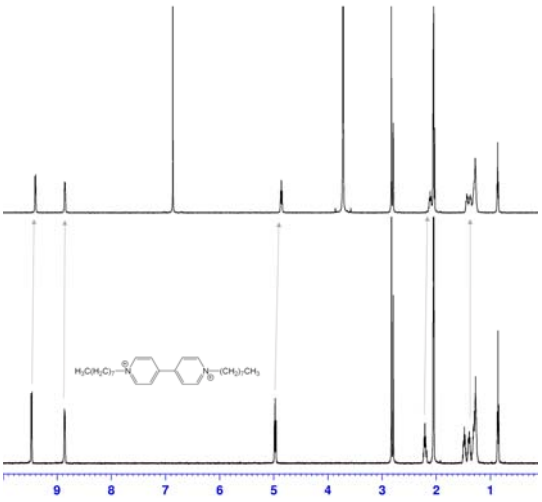

Figure S25. ^{1}H NMR spectra of *N*,*N*'-dioctyl-4,4'-bipyridinium bishexafluorophosphate salt (4.9 mM, 500 MHz, $CDCl_3$) in the absence and presence of MeP5A host (4.4 mM). NMR results indicated that MeP5A did not form inclusion complex with the guest or at least had very weak interactions.

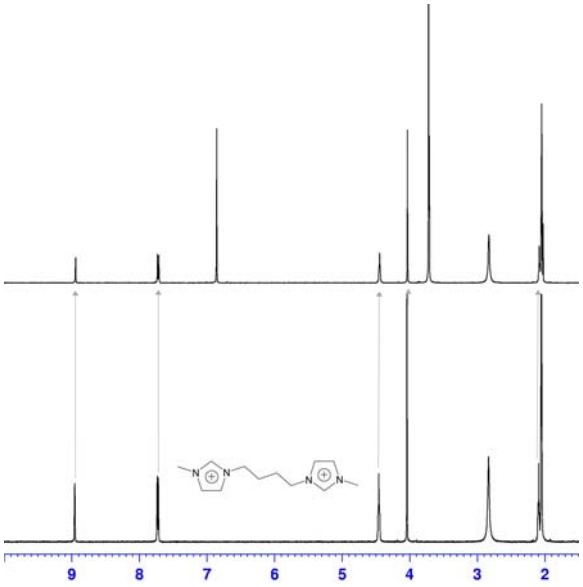

Figure S26. ^{1}H NMR spectra of bis(imidazolium)butane bishexafluorophosphate salt (4.8 mM, 500 MHz, $CDCl_3$) in the absence and presence of MeP5A host (4.0 mM). NMR results indicated that MeP5A did not form inclusion complex with the guest or at least had very weak interactions.

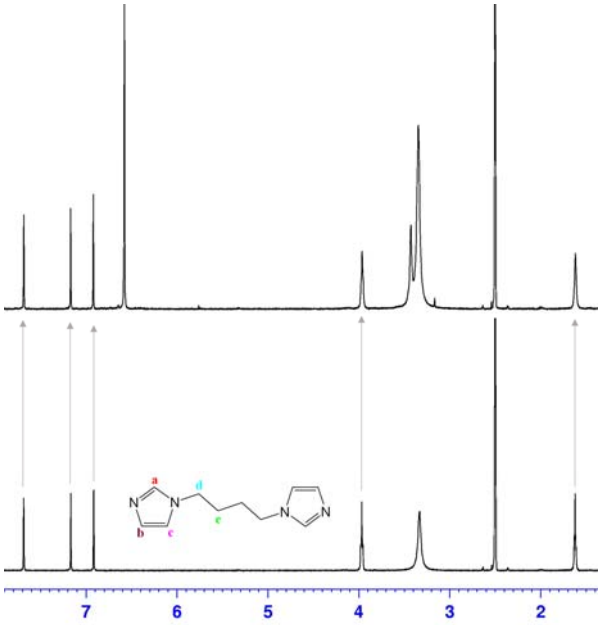

Figure S27. ^{1}H NMR spectra of BIMBu (4.8 mM, 500 MHz, DMSO-d_6) in the absence and presence of parent P5A host (5.0 mM). NMR results indicated that parent P5A did not form inclusion complex with the guest in DMSO-d_6 or at least had very weak interactions.

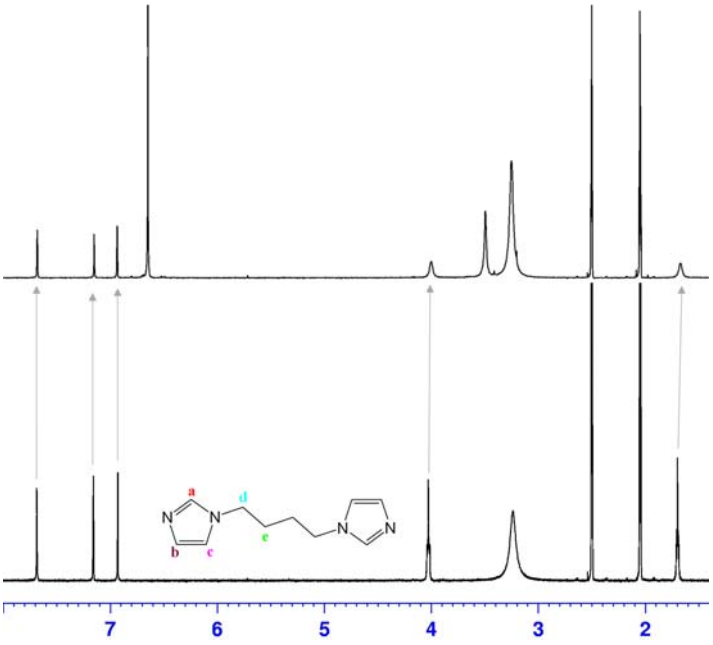

Figure S28. ^{1}H NMR spectrum (500 MHz) of BImBu (4.7 mM) in the absence (lower) and presence (upper) of parent P5A (5.1 mM) in 1 : 1 (v : v) acetone-d_6 : DMSO-d_6. NMR results indicated that parent P5A did not form inclusion complex with the guest in acetone-d_6/DMSO-d_6 or at least had very weak interactions.

2D NOESY analysis of BImBu with EtP5A.

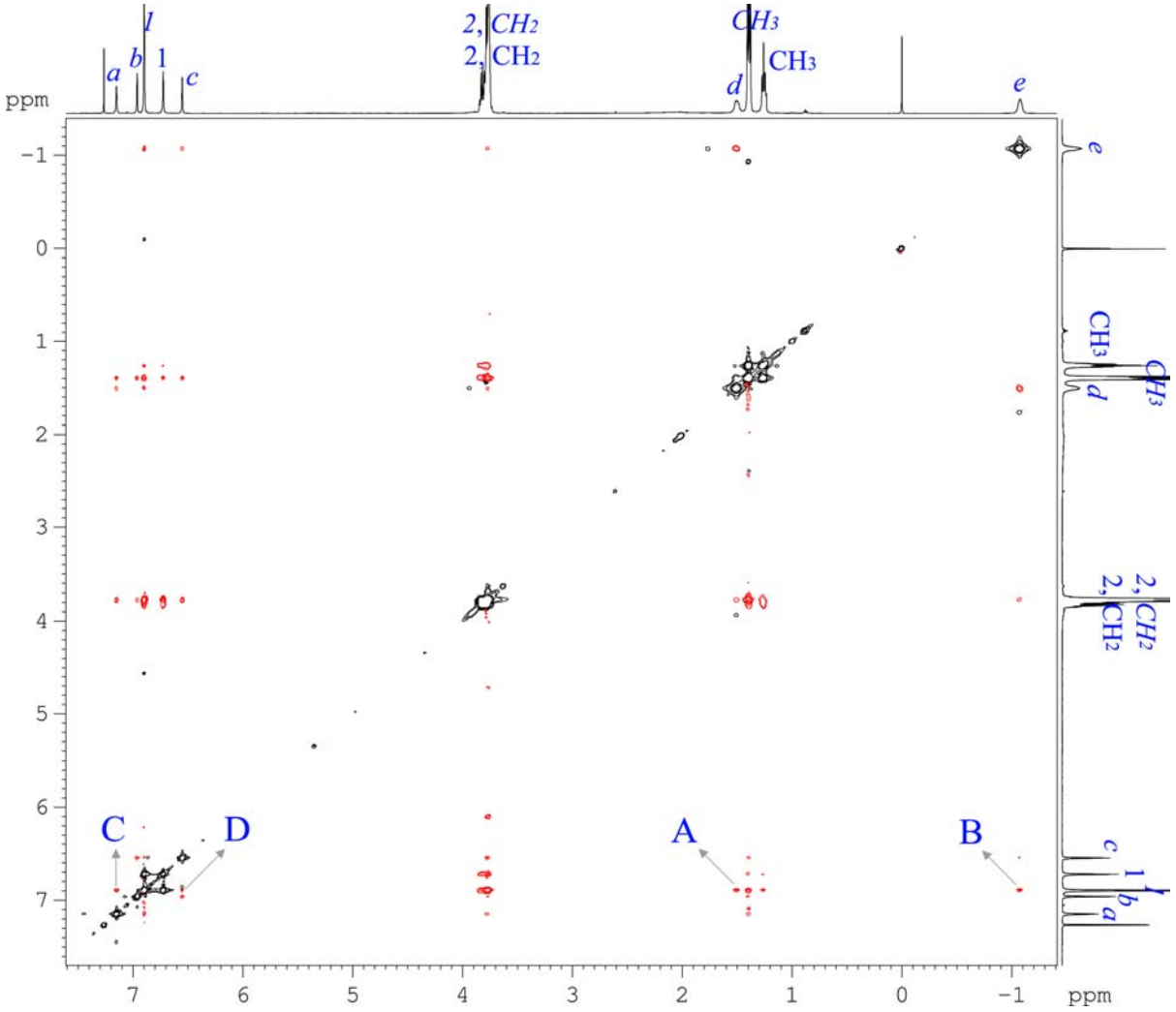

Figure S29. 2D NOESY analysis of BImBu with EtP5A in $CDCl_3$ with a mixing time of 200 ms. (500 MHz, 298 K, The concentrations of host and guest are 18.0 and 13.8 mM, respectively)

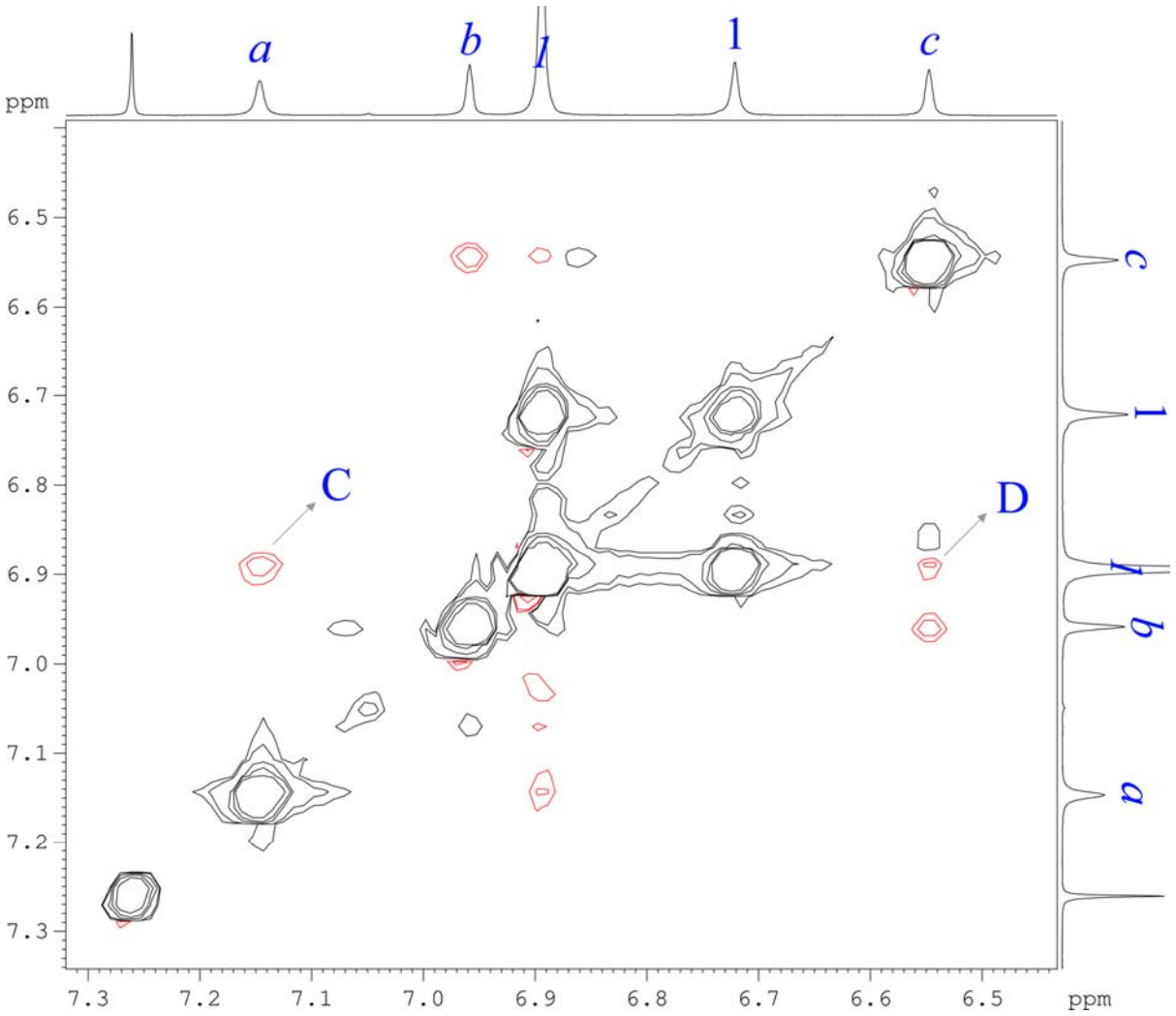

Figure S30. Partial 2D NOESY analysis of BImBu with EtP5A in $CDCl_3$ with a mixing time of 200 ms. (500 MHz, 298 K, The concentrations of host and guest are 18.0 and 13.8 mM, respectively)

X-ray crystal data and crystal structures of EtP5A host, and BImBu⊂EtP5A complex.

X-ray crystal data for EtP5A.

Crystallographic data: colorless, $C_{55}H_{76}O_{13}$, *FW* 945.16, Triclinic, space group *P-1*, a = 12.290 (5), b = 14.968 (6), c = 21.902 (8), α = 90.837 (5)°, β = 90.985 (5)°, γ = 105.028 (6)°, V = 3889.89(683) Å^3, Z = 8, D_c = 0.807 g cm^{-3}, T = 296(2)K, μ = 0.057mm^{-1}, 20358 measured reflections, 13554 independent reflections, 623 parameters, 6 restraint, F(000) = 1020, R_1 = 0.3605, wR_2 = 0.6369 (all data), R_1 = 0.2543, wR_2 = 0.5858 [I > 2σ(I)], max. residual density 1.851 e·Å^{-3}, and goodness-of-fit (F^2) = 1.935. CCDC 831702.

X-ray crystal data for BImBu⊂EtP5A.

Crystallographic data: colorless, $C_{65}H_{84}N_4O_{10}$, *FW* 1081.36, Monoclinic, space group P2(1)/n, a = 13.215 (2), b = 22.647 (4), c = 20.966 (4), α = γ = 90.00 °, β = 100.064 (3)°, V = 6178.16(378) Å^3, Z = 4, D_c = 1.163 g cm^{-3}, T = 296(2)K, μ = 0.078mm^{-1}, 31752 measured reflections, 10924 independent reflections, 699 parameters, 6 restraint, F(000) = 2328, R_1 = 0.1790, wR_2 = 0.2895 (all data), R_1 = 0.0866, wR_2 = 0.2308 [I > 2σ(I)], max. residual density 0.528 e·Å^{-3}, and goodness-of-fit (F^2) = 1.061. CCDC 831701.

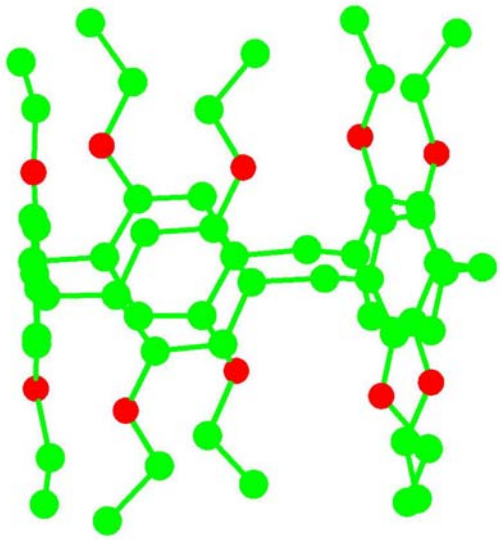

Figure S31. Crystal structure of EtP5A host. Hydrogens have been omitted for clarity. Carbons are green, and oxygens are red.

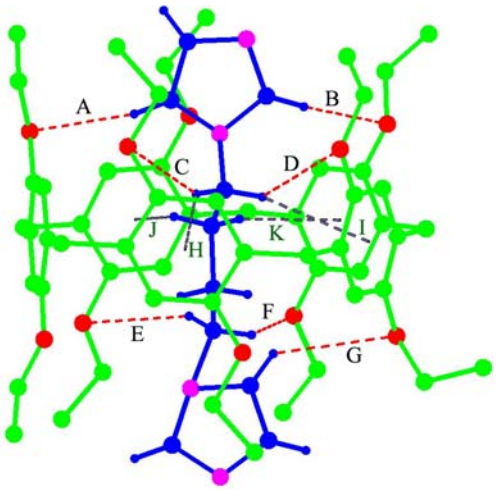

Figure S32. Crystal structure of the interpenetrated complex BImBu⊂EtP5A. Hydrogens of the host have been omitted for clarity. EtP5A is green, BImBu is blue, oxygens are red, and nitrogens are magenta. Red dashes represent C−H···O hydrogen bonds, and gray dashes represent C−H···π interactions. C−H···O hydrogen-bond parameters: H···O distances (Å), C−H···O angles (deg) A, 2.78, 141; B, 2.45, 156; C, 3.01, 152; D, 2.97, 139; E, 2.86, 149; F, 2.87, 130; G, 2.98, 130. C−H···π parameters: H···ring centre distances (Å), C−H···ring angles (deg) H, 2.68, 137; I, 2.75, 164; J, 3.06, 127; K, 3.00, 167.

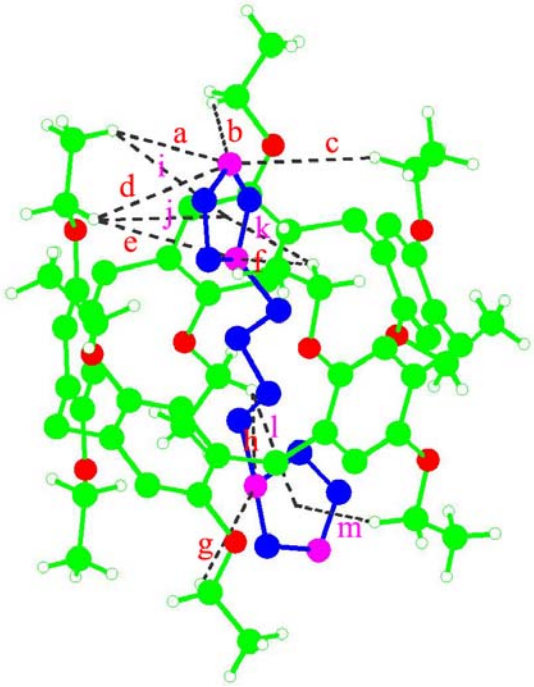

Figure S33. Crystal structure of the interpenetrated complex BImBu⊂EtP5A. Hydrogens of the guest have been omitted for clarity. EtP5A is green, BImBu is blue, oxygens are red, and nitrogens are magenta. Black dashes represent weak C−H···N hydrogen bonds or C−H···π interactions. C−H···N hydrogen-bond parameters: H···N distances (Å), C−H···N angles (deg) a, 3.28, 127; b, 3.42, 138; c, 3.39, 153; d, 3.44, 127; e, 3.37, 137; f, 3.42, 144; g, 3.66, 136; h, 3.80, 128; C−H···π parameters: H···ring centre distances (Å), C−H···ring angles (deg) i, 3.65, 117; j, 3.09, 142; k, 3.21, 149; l, 3.75, 141; m, 3.12, 140. Besides these weak C−H···N interactions and C−H···π interactions, there exist multiple C−H···O hydrogen bonding interactions (A−G), and multiple C−H···π interactions (H−K), as shown in Figure 32. These multiple noncovalent interactions certainly play an important role in the formation of the interpenetrated complex and its strong stability.

Determination of the association constants.

(1). For BImBu/BImPro/BImPen⊂AlkP5A host-guest complexes, chemical exchange is slow on the NMR time scale and peaks are observed for both complexed and uncomplexed species in the NMR spectra. So association constants for these complexes could be determined by integration from a 1 : 1 mixture using the ^{1}H NMR single point method.[3,4] (Table 1)

$$K_a = \frac{[P5A{\cdot}G]_c}{[P5A]_{uc}[G]_{uc}}$$

(2). For BuIm guest, chemical exchange is fast on the NMR time scale. To determine the association constant, NMR titrations were done with solutions which had a constant concentration of EtP5A and varying concentrations of guest. Using the nonlinear curve-fitting method, the association constant was obtained for each host-guest combination from the following equation[5]:

$$A = (A_\infty/[P5A]_0)\ (0.5[G]_0 + 0.5([P5A]_0+1/K_a) - (0.5\ ([G]_0^2+(2[G]_0(1/K_a - [P5A]_0)) + (1/K_a + [P5A]_0)^2)^{0.5}))$$

Where A is the chemical shift change of H_1 on AlkP5A host at $[G]_0$, A_∞ is the chemical shift change of H_1 when the host is completely complexed, $[P5A]_0$ is the fixed initial concentration of the EtP5A host, and $[G]_0$ is the initial concentration of guest.

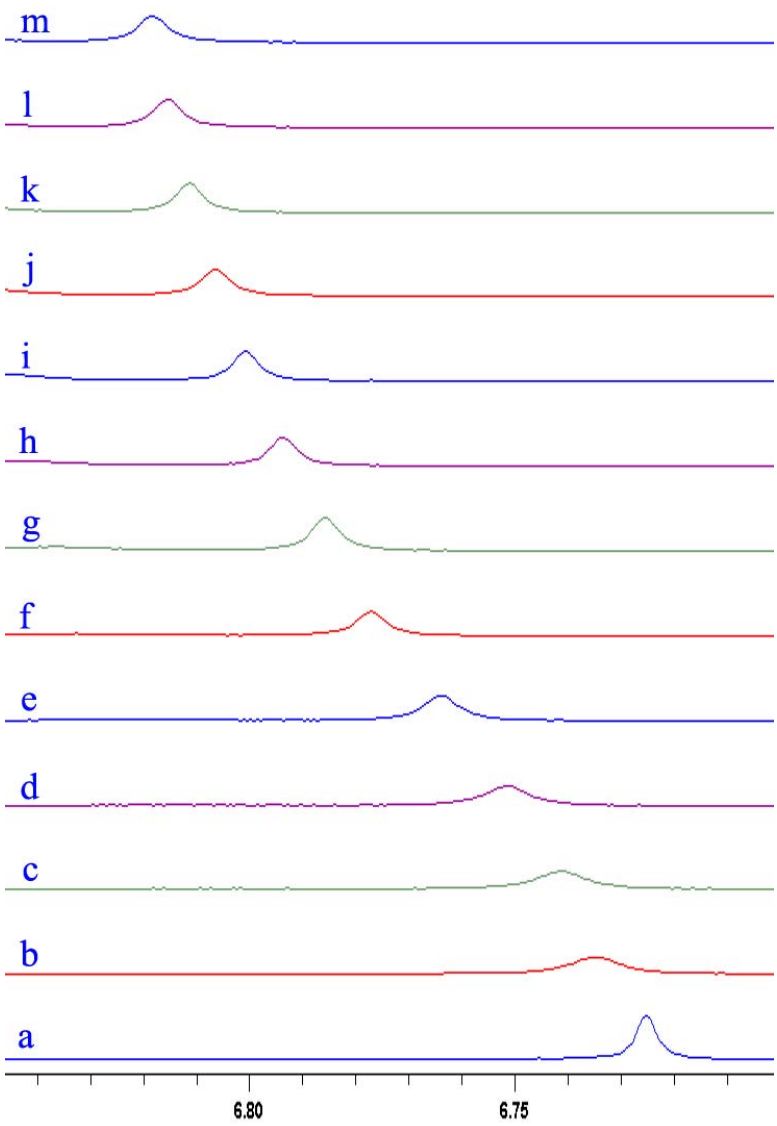

Figure S34. Partial ^{1}H NMR spectra (500 MHz, $CDCl_3$, 298 K) of EtP5A at a concentration of 1.0 mM upon addition of BImBu: (a) 0 mM, (b) 0.4 mM, (c) 1.1 mM, (d) 1.7 mM, (e) 2.6 mM, (f) 4.6 mM, (g) 5.4 mM, (h) 7.5 mM, (i) 9.8 mM, (j) 12.0 mM, (k) 14.6 mM, (l) 17.8 mM, and (m) 20.7 mM.

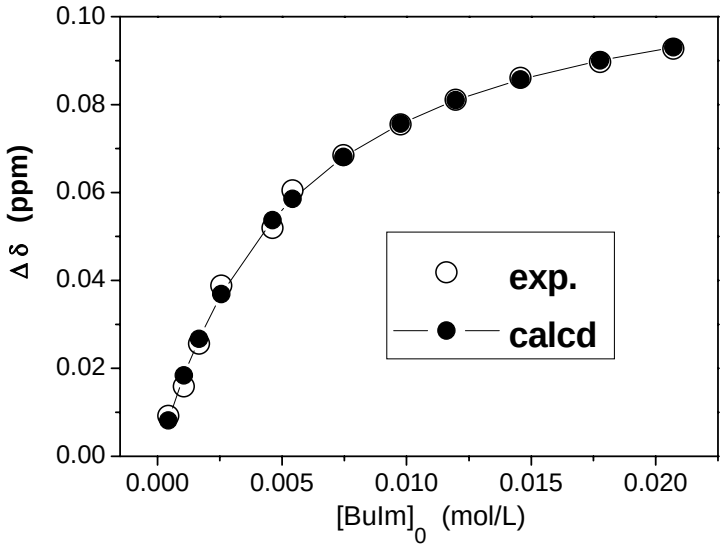

Figure S35. The non-linear curve-fitting (NMR titrations) for the complexation of EtP5A host (1.0 mM) with BImBu in $CDCl_3$ at 298 K. The concentration of BImBu was 0, 0.4, 1.1, 1.7, 2.6, 4.6, 5.4, 7.5, 9.8, 12.0, 14.6, 17.8, 20.7 mM.

The corresponding K_a values are listed in Table 1 in the manuscript.

(3). The association constant of BuIm with EtP5A have also been determined using the indirect method.[6] Guest BImPen (G_{ref}, see Fig. S22) that exhibits slow exchange kinetics and an excess of BuIm are allowed to compete for a limiting quantity of EtP5A. The association constants between G_{ref} and EtP5A are (7.9 ± 0.5) × 10^2 M^{-1} in $CDCl_3$ (Table 1). The integration of the resonances for the free and bound guest then allow for a calculation of the association constant. In the three component system:

$$K_{a\ ref} = \frac{[P5A{\cdot}G_{ref}]_c}{[P5A]_{uc}[G_{ref}]_{uc}}$$

$$\therefore\ [P5A]_{uc} = \frac{[P5A{\cdot}G_{ref}]_c}{[G_{ref}]_{uc}K_{a\ ref}}$$

So the unknown K_a could be determined using the following equation:

$$K_a = \frac{[P5A{\cdot}G]_c}{[P5A]_{uc}[G]_{uc}} = \frac{[P5A]_0 - [P5A]_{uc} - [P5A{\cdot}G_{ref}]_c}{[P5A]_{uc}([G]_0 - [P5A{\cdot}G]_c)}$$

$$= \frac{[P5A]_0 - [P5A]_{uc} - [P5A{\cdot}G_{ref}]_c}{[P5A]_{uc}\{[G]_0 - ([P5A]_0 - [P5A]_{uc} - [P5A{\cdot}G_{ref}]_c)\}}$$

As shown in Table S1, the K_a values for EtP5A with BuIm system determined using the indirect method are almost accordant with those from NMR titration.

TABLE S1. Association constant (K_a/M^{-1}) for complexation of EtP5A with BuIm in $CDCl_3$ at 298 K using different methods.

K_a [a]	K_a [b]
$(2.5\pm0.4) \times 10^2$	2.8×10^2

[a] NMR titration. [b] The indirect method.

Determination of thermodynamic parameters.

The association constants of the inclusion complexation of BImBu with four AlkP5A hosts were determined via NMR single point method at various temperatures ranging from 272.9 K to 313.0 K, which were listed in Table S2. The complexation thermodynamic parameters ($\Delta H°$ and $\Delta S°$) were obtained by the slope and ordinate-intercept of van't Hoff analysis $\ln K_a \approx 1/T$ plots applying the following equation:

$$\ln K_a = -\frac{\Delta H}{RT} + \frac{\Delta S}{R}$$

The free energy ($-\Delta G°$), enthalpy ($-\Delta H°$), and entropy changes ($T\Delta S°$) for the host-guest complexation are listed in Table 2 in the manuscript.

TABLE S2: **Association Constants (log K_a) of Inclusion Complexation of AlkP5A with BImBu Guest in $CDCl_3$ at Various Temperature.**

Host	Temperature (K)	log K_a
MeP5A	273.0	4.04
	283.0	3.88
	298.0	3.67
	303.1	3.58
	313.0	3.45
EtP5A	273.0	4.86
	282.8	4.60
	298.0	4.30
	303.0	4.19
	313.0	3.98
BuP5A	272.9	4.71

	283.0	4.46
	298.0	4.18
	303.0	4.04
	313.0	3.91
Octp5A	273.0	4.26
	283.0	4.08
	298.0	3.87
	303.1	3.79
	313.0	3.61

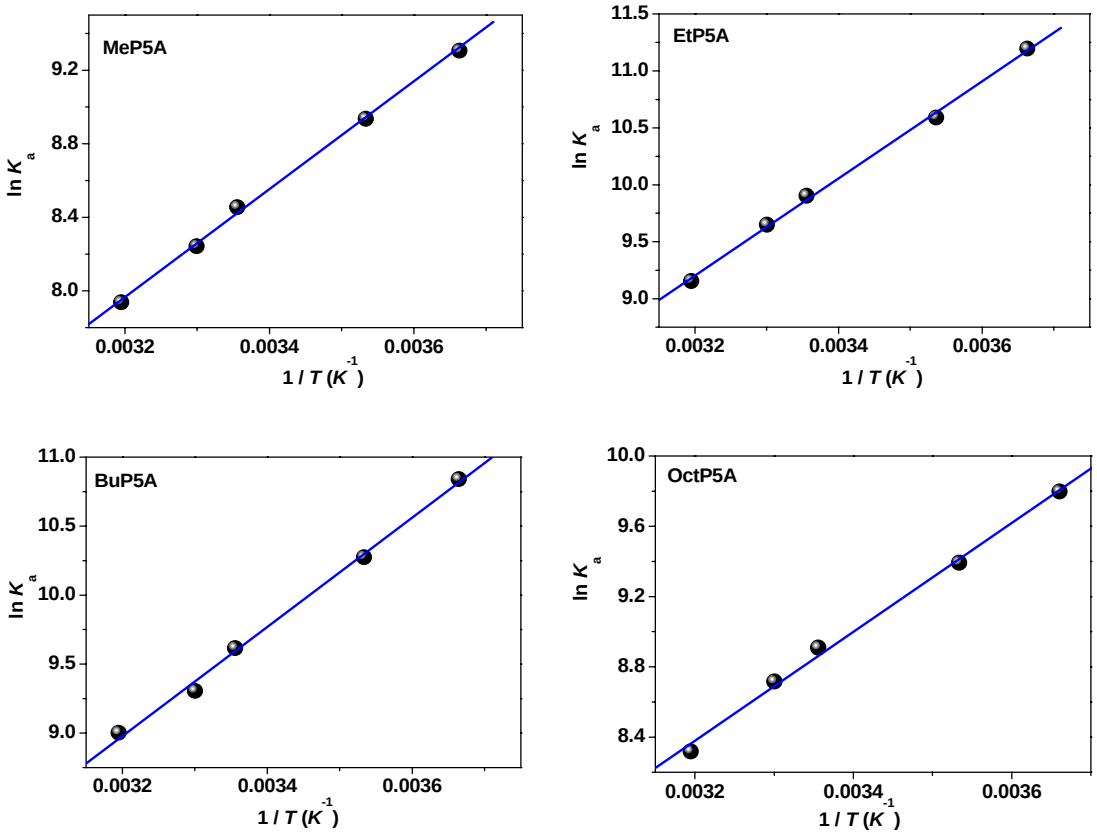

Figure S36. The plot of lnK_a versus 1/T for the complexation of AlkP5As with BImBu guest.

References.

S1 J.-F. Ma, J. Yang, G.-L. Zheng, L. Li, J.-F. Liu, *Inorg. Chem.* **2003**, *42*, 7531–7534.

S2 T. Ogoshi, S. Kanai, S. Fujinami, T. Yamagishi, Y. Nakamoto, *J. Am. Chem. Soc.* **2008**, *130*, 5022–5023.

S3 J. C. Adrian, Jr., C. S. Wilcox, *J. Am. Chem. Soc.* **1991**, *113*, 678–680.

S4 Association constants determined using the ^{1}H NMR single point methods. See: (a) A. B. Braunschweig, C. M. Ronconi, J.-Y. Han, F. Arico, S. J. Cantrill, J. F. Stoddart, S. I. Khan, A. J. P. White, D. J. Williams, *Eur. J. Org. Chem.* **2006**, 1857–1866.; b) S. J. Loeb, J. A. Wisner, *Angew. Chem. Int. Ed.* **1998**, *37*, 2838–2840; c) S. J. Loeb, J. Tiburcio, S. J. Vella, *Org. Lett.* **2005**, *7*, 4923–4926; d) J.-M. Zhao, Q.-S. Zong, T. Han, J.-F. Xiang, C.-F. Chen, *J. Org. Chem.* **2008**, *73*, 6800–6806; e) L. Li, G. J. Clarkson, *Org. Lett.*, **2007**, *9*, 497–500; f) D. Castillo, P. Astudillo, J. Mares, F. J. González, A. Vela, J. Tiburcio, *Org. Biomol. Chem.*, **2007**, *5*, 2252–2256; g) C. Li, Q. Xu, J. Li, F. Yao, X. Jia, *Org. Biomol. Chem.*, 2010, **8**, 1568–1576.

S5 a) K. A. Connors, Binding Constants; Wiley: New York, **1987**. Corbin, P. S. Ph.D. Dissertation, University of Illinois at Urbana-Champaign, Urbana, IL, 1999; b) R. P. Ashton, R. Ballardini, V. Balzani, M. Belohradsky, M. T. Gandolfi, D. Philp, L. Prodi, F. M. Raymo, M. V. Reddington, N. Spencer, J. F. Stoddart, M. Venturi , D. J. Williams, *J. Am. Chem. Soc.*, **1996**, *118*, 4931–4951; c) Y. Inoue, K. Yamamoto, T. Wada, S. Everitt, X.-M. Gao, Z.-J. Hou, L.-H. Tong, S.-K. Jiang, H.-M. Wu, *J. Chem. Soc., Perkin Trans. 2*, **1998**, 1807−1816.

S6 a) W. L. Mock, N. Y. Shih, *J. Org. Chem.* **1986**, *51*, 4440–4446; b) S. Liu, C. Ruspic, P. Mukhopadhyay, S. Chakrabarti, P. Y. Zavalij, L. Isaacs, *J. Am. Chem. Soc.*, **2005**, *127*, 15959–15967; c) R. E. Heath, G. M. Dykes, H. Fish, D. K. Smith, *Chem. Eur. J.*, **2003**, *9*, 850–855.